Colloid Polym Sci 275:474–479 (1997)

ORIGINAL CONTRIBUTION

M. Fujiwara
T. Okano
T.-H. Nakashima
A.A. Nakamura
G. Sugihara

A temperature study on critical micellization concentration (CMC), solubility, and degree of counterion binding of α-sulfonatomyristic acid methyl ester in water by electroconductivity measurements

Received: 28 August 1996
Accepted: 5 November 1996

M. Fujiwara · T. Okano
Lion Co.
Surf. Science Research Center
13-12 Hirai 7-chome
Edgawa-ku
Tokyo 123, Japan

T.-H. Nakashima · A.A. Nakamura
Prof. Dr. G. Sugihara (✉)
Fukuoka University
Department of Chemistry
Jonan-ku
Fukuoka 814-80, Japan

Abstract For a sodium salt of α-sulfonatomyristic acid methyl ester (14SFNa), one of the α-SFMe series surfactants, critical micellization concentration (CMC), solubility and degree of counterion binding (β) were determined by means of electroconductivity measurements at different temperatures (at every 5 °C) ranging from 15 to 50 °C. The phase diagram of 14SFNa in pure water was constructed from the CMC- and solubility-temperature data, in which the Krafft temperature (critical solution temperature) was found around 0 °C. The changes in the Gibbs energy, ΔG^0_m, enthalpy, ΔH^0_m, and entropy, ΔS^0_m, upon micelle formation as a function of temperature were evaluated taking β values into calculation.

Key words Critical micellization concentration (CMC) – solubility – degree of counterion binding – Krafft point – α-sulfonatomyristic acid methyl ester

Introduction

α-Sulfonate fatty acid methyl esters (α-SFMe) have been paid attention to their relatively quick availability from renewable vegetable material in addition to their good biodegradability [1–4]. We have been so far aquatinted with their superior detergency for fabrics [1, 5–7] as well as their high tolerance against calcium ions [1, 8].

Further, α-SFMe surfactants are well known to have a higher ability of emulsification compared with other surfactants; especially in the lower concentration its ability is far superior to the others [5]. Related to the superior performance in emulsification, the present authors, recently, reported a light-scattering study on the micellar systems solubilizing oleic acid in comparison of α-SFMe with sodium linear C_{12}/C_{14}-alkylbenzensulfonate (LAS). From this study it was found that α-SFMe forms a twice larger mixed micelles (or oleic acid-solubilizing micelles) compared with LAS and that the solubilizing process accompanies a reconstitution of the micelles, suggesting that the microenvironmental factor around the hydrophilic group plays a primarily important role [1, 8].

Focusing our attention on the aspect of surfactant properties caused by the head groups and/or counterion species, some of the present authors have revealed that counterion species affect much thermodynamic properties such as critical micellization concentration (CMC), solubility and Krafft temperature. Above all, the mixing effect of ionic–nonionic surfactants [9–11] as well as the dependency on counterion species [12, 13] has been found to be conspicuous, suggesting that the performances in the application aspects such as solubilization or emulsification, wetting, detergency, etc., are governed by the hydrophilic moiety including counterions.

As for the basic physicochemical properties of α-SFMe series, Schambil and Schwurger [6] and Fujiwara et al. [8] have shown the basic data of the Krafft point, solubility, aggregation number, etc. Further, there have so far appeared several studies on two series of systematically

CPS 796

modified α-sulfonated fatty acid esters, i.e. structural effects of α-sulfonated fatty acid esters [$C_mH_{2m+1}CH(SO_3Na)COOC_nH_{2n+1}$, $m = 8$–16 and $n = 8$–18] on surface-active properties and emulsion ability [14a], and on some other important aspects related to monolayer [14b], bilayer membrane [14c] and microemulsion [14d] formations. In addition to these studies, recently, Okano et al. have reported the detail in solution behavior of α-sulfonated fatty acid polyethylene glycol monoesters [$C_mH_{2m+1}CH(SO_3Na)COO(C_2H_4O)_nH$] and diesters [$C_mH_{2m+1}CH(SO_3Na)COO(C_2H_4O)_nCOCH(SO_3Na)C_mH_{2m+1}$] where $m = 10$–16 and $n = 1$–35 [15] in terms of Krafft point, CMC, interfacial tension, etc. However, no thermodynamic analysis has been made yet, so in the present paper thermodynamic behaviors are investigated for α-sulfonatomyristic acid methyl ester (14SFNa) based on the CMC and solubility data which were determined from electroconductivity measurements.

Experimentals

Materials and apparatus

Sodium salt of α-sulfonatomyristic acid methyl ester (14SFNa) was prepared similarly to the previous paper [8] (according to the method by Stirton et al. [16], and highly purified by repeated recrystallization from ethanol by the addition of slight amount of water. Sodium chloride as an added salt (from Nacalai Tesque Co. Kyoto) was of analytical grade and used as received. The electroconductivity measurement was carried out in the same manner as in the previous reports [12, 13] using a TOA Electric Conductivity Meter, Model CM-40S, together with a spouted cylinder type cell combined with a TOA Electrode (CG-201PL). A 250 μl Hamilton Microsyringe was used for injecting the sample solution through the spout; 15 cm^3 of solvent (pure water or aqueous solution of NaCl at each concentration) was initially contained in the cell.

Determinations of CMC and degree of counterion binding (β)

All of the CMC data were obtained from electroconductivity measurement. CMC in pure water was determined from conventional plots of specific conductivity (κ) vs. analytical concentration (C) at 5 °C, and at the temperatures ranging from 15 to 50 °C (at every 5 °C). Here, it is noted that in order to determine CMC in molality for convenience of thermodynamic analysis, the density of the prepared solution was preliminarily measured.

In the systems containing added salt, we applied the plot of the derivative ($d\kappa/dC$) against $\sqrt{C}$ where $d\kappa/dC$ was assumed as being equal to $\Delta\kappa/\Delta C$ ($\Delta\kappa = \kappa_{i+1} - \kappa_i$ and $\Delta C = C_{i+1} - C_i$ at "i"th measured point, and $\bar{C} = (C_{i+1} - C_i)/2$). For simplicity, $\bar{C}$ will be denoted as C hereafter in this text. The stock solutions with added NaCl were prepared using aqueous NaCl solutions at the respectively fixed concentrations. The β values were determined at the same temperatures as for CMC determination; the respective temperatures were controlled within ± 0.02 °C by the use of a thermostated water bath.

Solubility and Krafft point measurements

Solubility was also determined by means of conductivity measurement. The respective 14SFNa solutions were slowly cooled under a continuous stir by using an Acrobat Stirrer (MS KiKi Co.) with a rotor. Then the time course of their specific conductivity was observed and recorded; observing the slow decrease in κ accompanied by cooling, at a temperature, the κ value is found to start a rapid fall. The temperature giving the break in the κ vs. time (t) relation (accordingly, the break in the κ vs. temperature plot) is regarded as that at which the solution is saturated with 14SFNa, meaning that the concentration of the solution is the solubility itself at the temperature.

Results

The more accurate determination of CMC was found to be made from the plot of differential conductivity ($d\kappa/dC$) vs. square root of concentration in mM ($\sqrt{C}$) as compared with the conventional plot of specific conductivity (κ) vs. concentration (C), especially, for the systems with addition of NaCl. As is shown in Fig. 1, the curve has an abrupt fall drawing a reverse sigmoid, the center of which is regarded as the point giving CMC, based on the definition by Philips [17–19]. The differential conductivity has been applied to CMC determination by a few authors [20, 21] but in their application $d\kappa/dC$ was plotted against C [20, 21]. (Manabe et al. have determined CMC at the shoulder point of the $d\kappa/dC$ vs. C plot curve [21, 22].) In the present study, however, not only for drawing more clearly the reverse sigmoid but also for utilizing the conductivity data to determine the limiting molar conductance (Λ^0) in addition to micelllar conductance (Λ^M), the differential conductivity was plotted against $\sqrt{C}$ as has been applied in the previous study [17]. The treatment with the conductivity data will be discussed elsewhere [23].

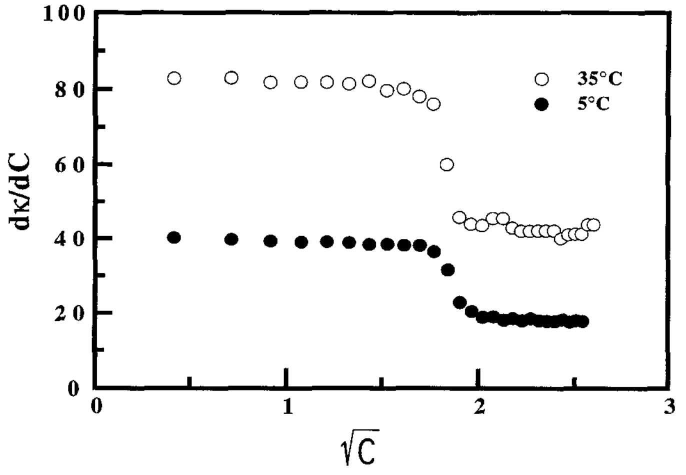

Fig. 1 Plots of differential conductivity vs. square root of concentration for 14SFNa in pure water at 5 and 30 °C. Each CMC is determined at the central point of the reverse sigmoid

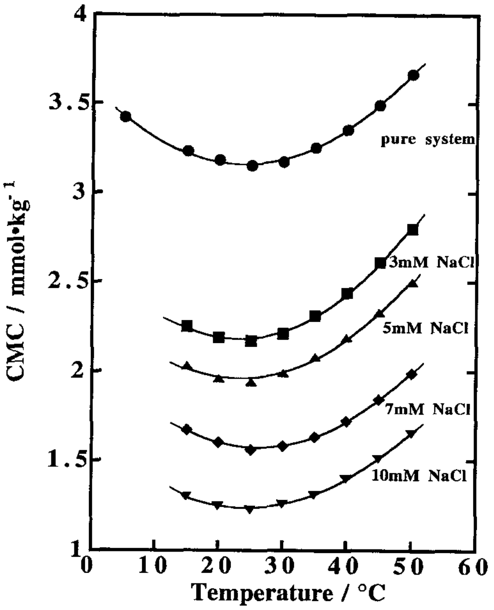

Fig. 2 The temperature dependence of CMC for 14SFNa at different concentrations of added NaCl. The CMC data are used for determining β at each temperature by the Corrin–Harkins plot

In Fig. 2 are shown the temperature changes of CMC determined by the above method as a function of added salt concentration. All the curves have a minimum around 28 °C as observed for different ionic surfactants [18, 24–28]. From Fig. 2 is clearly seen the added salt effect on CMC, although the concentration of the added salt is restricted to a narrow range below 10 mM.

The curves are used for estimating the degree of counterion binding to micelles (β) at each temperature; the β is given from the following relations:

$$\Delta G_m^0 = RT \ln X_{cmc}(X_{cmc} + X_a)^{\beta} \quad (1)$$

or

$$\ln X_{cmc} = \frac{\Delta G_m^0}{RT} - \beta \ln(X_{cmc} + X_a) \, , \quad (2)$$

where ΔG_m^0 is the standard Gibbs energy change upon micelle formation, X_{cmc} and X_a are concentrations in mole fraction of the surfactant at CMC and of the added salt in aqueous media, respectively, and RT is the product of the molar gas constant with the Kelvin temperature. From Eq. (2) the CMC as a function of added salt concentration is more concisely expressed as: $\ln \mathrm{CMC} = \mathrm{const}\,(T, P) - \beta \ln C_g$.

This equation indicates that the β corresponds to the slope of the curve in the plot of logarithmic CMC against logarithmic counterion (gegenion) concentration, i.e. $C_g = \mathrm{CMC} + \mathrm{concn.\ of\ added\ salt}$; this is the so-called Corrin–Harkins plot. These plots showed a good linearity with a regression of more than 0.98 at each temperature. Being plotted against temperature, the β increases a little and then decreases beyond a maximum with increased temperature (not shown here). The β values thus determined from the slopes and the CMC data (in milimolality) of the systems in pure water at the respective temperatures are tabulated in Table 1.

Table 1 The data of CMC and degree of counterion binding β at discrete temperatures

T [°C]	CMC [mmol kg^{-1}]	β
5	3.42	
15	3.23	0.716
20	3.18	0.717
25	3.15	0.716
30	3.17	0.715
35	3.25	0.713
40	3.35	0.710
45	3.49	0.707
50	3.67	0.702

Turning our attention to the solubility of 14SFNa, which was determined by means of electroconductivity measurements as described in the experimental section, the data were obtained at the lower temperature as compared with the data of previous study [8]. The abrupt change in conductivity with lowering temperature was observed at the lower temperature in contrast to the previous results determined visually on the heating process from a frozen solution containing 14SFNa crystalline precipitates. The

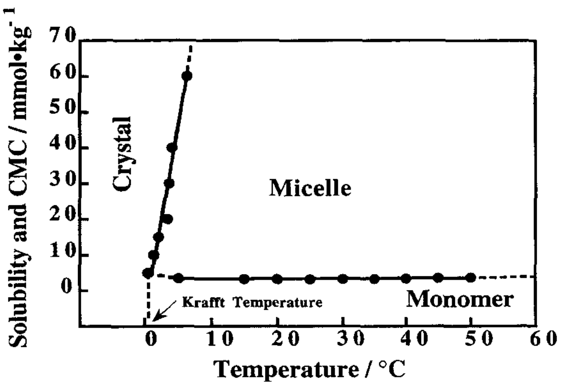

Fig. 3 The phase diagram of 14SFNa in water

present results, thus, led to the Krafft point at the lower temperature than the previous data visually determined. As shown in Fig. 3, a phase diagram at 1 atm was constructed; the intersection of solubility curve with CMC curve is likely to exist around 0 °C.

Discussion

The phase diagram given in Fig. 3 indicates the Krafft point around 0 °C which is lower than that of the previous study by 5 °C (see Fig. 1 in Ref. [8]) but the CMC values are higher, e.g. the CMC value of the previous paper is 2.8 at 13 °C while that of the present study apparently seems to be higher than 3.23 at 15 °C. The difference in the results may be ascribed to that in the employed approaches, suggesting that the dissolution from crystal state and the precipitation from solution state are rate-limiting process accompanying a kind of supersaturation or retardation phenomenon. The fact that CMC could be determined even at 5 °C (see Fig. 1) means that the Krafft point is lower than 6 °C. It is noted that the cooling method was employed for the determination of solubility in contrast to the previous heating method; the present result may involve a possibility that supercooling took place. Anyway the Krafft point of 14SFNa is practically considered to be between 0 and 6 °C and the phase diagram at least tells us that 14SFNa has a wide micellar region being suitable for common use.

Next, on the basis of the data in Table 1, let us try a thermodynamic analysis and discussion. First, the Gibbs energy change upon micelle formation should be examined. Applying the following equation derived from Eq. (1) when no salt is added ($X_a = 0$), the standard Gibbs energy change can be calculated using the basic data in Table 1:

$$\Delta G^0_m = (1 + \beta)RT \ln X_{cmc} \ . \qquad (3)$$

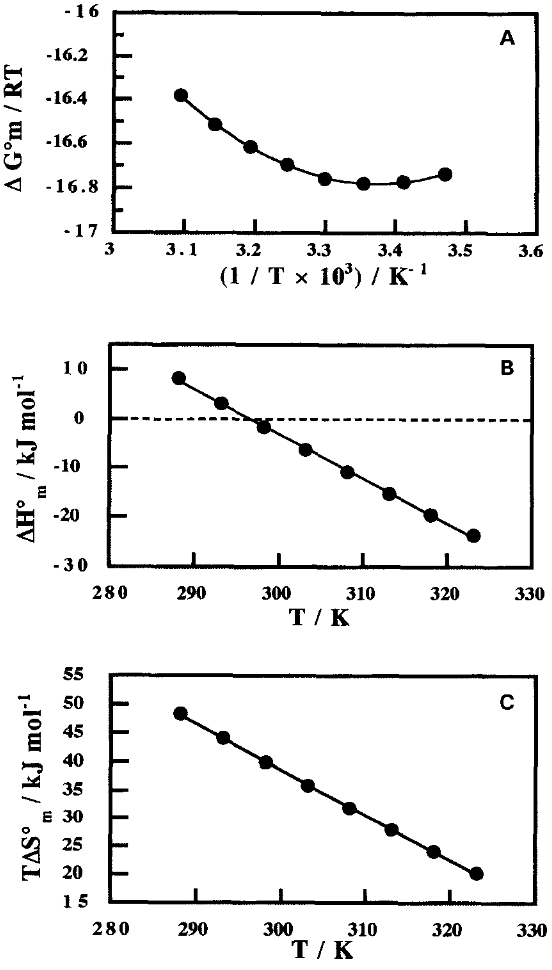

Fig. 4 Thermodynamic parameters as a function of temperature. **A** The van't Hoff plot based on the data in Table 1. **B** The enthalpy change ΔH^0_m upon micelle formation. **C** The entropy term calculated from the relation $T\ \Delta S^0_m = \Delta H^0_m - \Delta G^0_m$

Here it is well known that, strictly describing, this equation is derived from the charged phase-separation model [28] and Eq. (3) must be given with a different expression based on the mass action model [18, 29], but both models lead to the same expression when the aggregation number of micelles is greater than several tens [18]. The previous light scattering study has shown that the aggregation number of α-SFMe is several tens so that the Eq. (3) satisfies simultaneously the mass action model within a good approximation.

The well-known van't Hoff plot was applied for evaluating the enthalpy change on micelle formation ΔH^0_m from the Gibbs energy change; the obtained curve is shown in the top frame (A) of Fig. 4. Here, the product of the slope with the gas constant corresponds to the enthalpy change

Table 2 Thermodynamic parameters at various temperature

T [°C]	$-\Delta G^0_{\rm m}$ [kJ mol^{-1}]	$\Delta H^0_{\rm m}$ [kJ mol^{-1}]	$\Delta S^0_{\rm m}$ [JK^{-1} mol^{-1}]
15.0	40.1	8.28	168
20.0	40.9	3.24	150
25.0	41.6	− 1.63	134
30.0	42.2	− 6.35	118
35.0	42.8	− 10.9	103
40.0	43.3	− 15.3	89.2
45.0	43.7	− 19.6	75.7
50.0	44.0	− 23.7	62.7

as follows:

$$\left[\frac{\partial(\Delta G^0_{\rm m}/RT)}{\partial(1/T)}\right]_p = \frac{\Delta H^0_{\rm m}}{R} . \tag{4}$$

Further, using the estimated $\Delta H^0_{\rm m}$ value, the entropy change, $\Delta S^0_{\rm m}$, can be calculated from the relation $\Delta S^0_{\rm m} = (\Delta H^0_{\rm m} - \Delta G^0_{\rm m})/T$.

In the middle frame (B) and the bottom frame (C) of Fig. 4, $\Delta H^0_{\rm m}$ and the entropy term $T\,\Delta S^0_{\rm m}$ are plotted against the Kelvin temperature, respectively. Figure 4 shows that the enthalpy term changes from positive (endothermic) to negative (exothermic) at the temperature corresponding to the minimum of the CMC–temperature curve; on the other hand, the entropy term decreases monotonously with temperature (see Table 2).

As for the calculation of enthalpy change, the equation which has been used in the charged phase-separation model [25] is

$$\Delta H^0_{\rm m} = -(1+\beta)RT^2(\partial \ln {\rm CMC}/\partial T)_p . \tag{5}$$

This equation excludes the differential term of β with temperature, meaning that the Gibbs–Helmholts relation was applied by neglecting the temperature dependence of β. However, it has been pointed out that it is necessary to take into consideration not only the temperature variation of the CMC but that of β as well for calculating enthalpy change [26, 29]. Since changes in β in the mass action model are incorporated into $\Delta G^0_{\rm m}$ values at different temperatures, $\Delta H^0_{\rm m}$ can be readily determined from the slope $\Delta G^0_{\rm m}/RT$ vs. $1/T$ plot as is given in Fig. 4A. This plot has been known to be superior to that of the charged phase-separation model (Eq. (5)) [26, 29], so that the temperature dependence of β value was precisely determined to be applied to the calculation of $\Delta H^0_{\rm m}$ and $\Delta S^0_{\rm m}$ in the present study. The general trends of temperature dependence in $\Delta H^0_{\rm m}$ and $\Delta S^0_{\rm m}$ values with temperature found for 14SFNa are qualitatively consistent with those for hydrocarbon surfactants [27, 30–32] and even for a fluorocarbon surfactant [26]. That is, the contribution of entropy term to the Gibbs energy of micelle formation plays the leading part, especially in the lower-temperature region (below the minimum point on the CMC–temperature curve) while the contribution from enthalpy term increases with increasing temperature above the minimum point.

With respect to the variations of the entropy and enthalpy with temperature we discussed in more detail based on the present data of β (degree of counterion association onto micelles) or degree of micellar dissociation (α, where $\alpha + \beta$ was regarded as unity) in the separate paper [23]; in that the equilibrium between counterions in bulk solution and dissociated micelles was studied as a function of temperature. From the temperature dependence of the equilibrium, the enthalpy change of counterion association was determined as + 9.48 and − 8.56 kJ mol^{-1} at the respective temperature ranges below and above 28.4 °C (around the minimum of the CMC–temperature curve). The endothermic enthalpy change and the positive entropy change at the lower temperature were interpreted in terms of dehydration of ions when ionic association (counterion binding) takes place, the free ions having strongly bound water molecules of highly ordered structure release such water molecules accompanying heat absorption and increased randomness [33]. In the higher temperature range above ca. 28 °C, in contrast, the energetical stabilization between negatively and positively charged ions results in heat releasing [23]. By way of caution, here, the free energy change and the other parameters discussed at present are different from those upon micelle formation evaluated at CMC not only in the standard chemical potential but in the viewpoint. However, the temperature change in enthalpy term concerning the equilibrium between counterions and head groups can be closely related to that of micelle formation as is demonstrated in Fig. 4.

Acknowledgment The authors are grateful to Dr. Ohbu and coworkers in Lion Surf. Sci. Cent. and Drs. Lee and Nagadome, Fukuoka University, for supporting our research. This material was in part based on the funds from Fukuoka University Central Research Institute and from the Kim Man-Yu Foundation of Science Promotion.

References

1. Yoneyama Y (1995) J Jpn Oil Chem Soc (Yukagaku) 44:2
2. Maurer EW, Weil JK, Linfieked WM (1977) J Am Oil Chem Soc 54:582
3. Steber J, Wierrich D (1989) Tenside Surf Deter 26:406

4. Masuda M, Odake H, Miura K (1994) J Jpn Oil Chem Soc (Yukagaku) 43:617
5. Okumura O, Sakatani, Yamane I (1976) 7th Comite International des Derives Tensio-Actis Moscow,Vol 1, p 25
6. Schambil F, Schuwuger MJ (1990) Tenside Surf Deter 27:380
7. Satsuki T, Umehara K, Yoneyama Y (1992) J Am Oil Chem Soc 69:672
8. Fujiwara M, Miyake M, Abe Y (1993) Colloid Polym Sci 271:780
9. Sugihara G, Yamamoto Y, Wada Y, Murata Y, Ikawa Y (1988) J Solution Chem 17:225
10. Sugihara G (1989) In: Mittal KL (ed) Surfactants in Solution, Vol 7. Plenum, New York, p 397
11. Wada Y, Ikawa Y, Igimi H, Murata Y, Nagadome S, Sugihara G (1990) J Jpn Oil Chem Soc (Yukagaku), 39:548
12. Sugihara G, Nagadome S, Yamashita T, Kawachi N, Takagi H, Moroi Y (1991) Colloids Surf 61:111
13. Sugihara G, Arakawa Y, Tanaka T, Lee S, Moroi Y (1995) J Colloid Interface Sci 170:399
14. (a) Okano T, Tanabe J, Fukuda M, Tanaka M (1992) J Am Oil Chem Soc 69:44; (b) Abe M, Okuma Y, Kwon KO, Okano T, Tanabe J, Fukuda M (1993) J Jpn Oil Chem Soc 42:447; (c) Abe M, Okuma Y, Kwom KO, Ogino K, Okano T, Tanabe J, Fukuda M (1993) J Jpn Oil Chem Soc 42:929; (d) Hiraro Y, Okano T, Murata S, Urabe S, Abe M (1995) J Jpn Soc Colour Material 68:149
15. Okano T, Egawa N, Fujiwara M, Fukuda M (1996) J Am Oil Chem Soc 73:31
16. Stirton AJ, Bistline RG, Jr, Weil JK, Waldo CA, Maurer EW (1962) J Am Oil Chem Soc 39:128
17. Sugihara G, Era Y, Funatsu M, Lee S, Sasaki Y, in press
18. Moroi Y (1992) In: Micelles–Theoretical and Applied Aspects Ch. 4. Plenum, New York
19. Moroi Y, Matuura R (1988) Bull Chem Soc Jpn 61:333
20. Mukerjee P, Yang AYS (1976) J Phys Chem 80:1388
21. Manabe M, Kawamura H, Yamashita A, Tokunaga S (1987) J Colloid Interface Sci 115:147
22. Manabe M, Kawamura H, Yamashita Y, Tokunaga S (1990) In: Bloor M, Wyn-Jones E (eds) The Structure, Dynamics and Equilibrium Properties of Colloidal Systems, p 63
23. Sugihara G, Nakamura AA, Nakashima T-H, Araki T-I, Okano T, Fujiwara M, to be submitted
24. Goddard ED, Benson GC (1957) Can J Chem 35:986
25. Shinoda K, Katsura K (1964) J Phys Chem 68:1568
26. Mukerjee P, Korematsu K, Okawauchi M, Sugihara G (1985) J Phys Chem 89:5308
27. Sugihara G, Arakawa Y, Tanak K, Lee S, Moroi Y (1995) J Colloid Interface Sci 170:399
28. Shinoda K (1963) In: Shinoda K, Nakagawa T, Tamamushi B-I, Isemura T (eds) Colloidal Surfactants, Ch. 1. Academic Press, New York
29. Mukerjee P (1996) Adv Colloid Interface Sci 21:331
30. Musbally GM, Perron G, Desnoyers JE (1976) J Colloid Interface Sci 54:80
31. de Lisi R, Ostiguy C, Perron G, Desnoyers JE (1979) J Colloid Interface Sci 71:147
32. de Lisi R, Perron G, Desnoyers JE (1980) Can J Chem 58:359
33. Ohtaki H (1987) In: Youeki no Kagaku (Solution Chemistry) (Chem Soc Jpn Ed) Dainihom Tosho, Tokyo